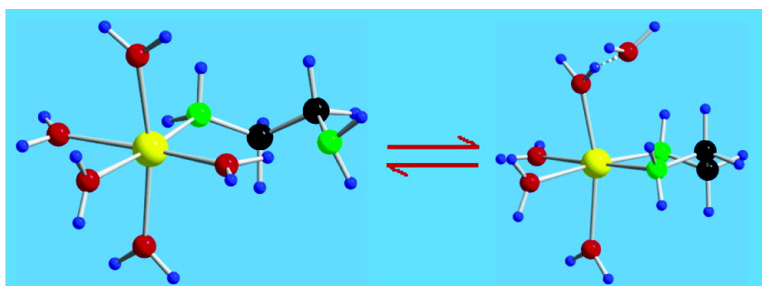


Chelate Effect and Thermodynamics of Metal Complex Formation in Solution: A Quantum Chemical Study

Valrie Vallet, Ulf Wahlgren, and Ingmar Grenthe

J. Am. Chem. Soc., **2003**, 125 (48), 14941-14950 • DOI: 10.1021/ja036646j • Publication Date (Web): 11 November 2003

Downloaded from <http://pubs.acs.org> on March 30, 2009



More About This Article

Additional resources and features associated with this article are available within the HTML version:

- Supporting Information
- Links to the 8 articles that cite this article, as of the time of this article download
- Access to high resolution figures
- Links to articles and content related to this article
- Copyright permission to reproduce figures and/or text from this article

[View the Full Text HTML](#)

Chelate Effect and Thermodynamics of Metal Complex Formation in Solution: A Quantum Chemical Study

Valérie Vallet,^{*,†} Ulf Wahlgren,[‡] and Ingmar Grenthe^{*,§}

Contribution from the Institute of Physical and Theoretical Chemistry, Technical University of Munich, D-85747 Garching, Germany, AlbaNova University Center, Institute of Physics, Stockholm University, Stockholm, Sweden, and Inorganic Chemistry, Department of Chemistry, Royal Institute of Technology (KTH), S-10044 Stockholm, Sweden

Received June 12, 2003; E-mail: valerie.vallet@ch.tum.de; ingmarg@kth.se

Abstract: The accuracy of quantum chemical predictions of structures and thermodynamic data for metal complexes depends both on the quantum chemical methods and the chemical models used. A thermodynamic analogue of the Eigen–Wilkins mechanism for ligand substitution reactions (Model A) turns out to be sufficiently simple to catch the essential chemistry of complex formation reactions and allows quantum chemical calculations at the ab initio level of thermodynamic quantities both in gas phase and solution; the latter by using the conductor-like polarizable continuum (CPCM) model. Model A describes the complex formation as a two-step reaction: 1. $[M(H_2O)_x](aq) + L(aq) \rightleftharpoons [M(H_2O)_x]L(aq)$; 2. $[M(H_2O)_x]L(aq) \rightleftharpoons [M(H_2O)_{x-1}L](aq) + (H_2O)(aq)$. The first step, the formation of an outer-sphere complex is described using the Fuoss equation and the second, the intramolecular exchange between an entering ligand from the second and water in the first coordination shell, using quantum chemical methods. The thermodynamic quantities for this model were compared to those for the reaction: $[M(H_2O)_x](aq) + L(aq) \rightleftharpoons [M(H_2O)_{x-1}L](aq) + (H_2O)(aq)$ (Model B), as calculated for each reactant and product separately. The models were tested using complex formation between Zn^{2+} and ammonia, methylamine, and ethylenediamine, and complex formation and chelate ring closure reactions in binary and ternary UO_2^{2+} –oxalate systems. The results show that the Gibbs energy of reaction for Model A are not strongly dependent on the number of water ligands and the structure of the second coordination sphere; it provides a much more precise estimate of the thermodynamics of complex formation reactions in solution than that obtained from Model B. The agreement between the experimental and calculated data for the formation of $Zn(NH_3)^{2+}(aq)$ and $Zn(NH_3)_2^{2+}(aq)$ is better than 8 kJ/mol for the former, as compared to 30 kJ/mol or larger, for the latter. The Gibbs energy of reaction obtained for the UO_2^{2+} –oxalate systems using model B differs between 80 and 130 kJ/mol from the experimental results, whereas the agreement with Model A is better. The errors in the quantum chemical estimates of the entropy and enthalpy of reaction are somewhat larger than those for the Gibbs energy, but still in fair agreement with experiments; adding water molecules in the second coordination sphere improves the agreement significantly. Reasons for the different performance of the two models are discussed. The quantum chemical data were used to discuss the microscopic basis of experimental enthalpy and entropy data, to determine the enthalpy and entropy contributions in chelate ring closure reactions and to discuss the origin of the so-called “chelate effect”. Contrary to many earlier suggestions, this is not even in the gas phase, a result of changes in translation entropy contributions. There is no simple explanation of the high stability of chelate complexes; it is a result of both enthalpy and entropy contributions that vary from one system to the other.

Introduction

Quantum chemistry offers one possible method for discussing the microscopic basis of thermodynamics, i.e., interpreting macroscopic events in molecular terms. In this communication, we discuss the modeling of solution chemical equilibria using quantum chemical methods, including a discussion of the chelate effect for complex formation reactions in solution. The outline

is as follows: we begin with the presentation of a quantum chemical model for complex formation that is sufficiently simple to catch the essential chemistry, at the same time allowing calculation of thermodynamic quantities for such reactions in both gas phase and solution. To test the applicability of the model, we used two chemically very different model systems. The first describes the formation of complexes between Zn^{2+} and ammonia, methylamine, and ethylenediamine. The second complex formation and chelate ring closure reactions in different UO_2^{2+} –oxalate systems.

In the second part, we discuss experimental and theory based entropies of the reactants/products and some previous proposals

[†] Institute of Physical and Theoretical Chemistry, Technical University of Munich.

[‡] AlbaNova University Center, Institute of Physics, Stockholm University.

[§] Inorganic Chemistry, Department of Chemistry, Royal Institute of Technology.

to explain the high stability of chelate complexes; finally we will discuss the thermodynamics of chelate ring closure/ring opening reactions.

It is well-known that the equilibrium constant for complex formation reactions of the type



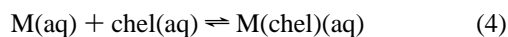
is much larger for multidentate ligands than for unidentate. One suggested explanation^{1–3} of this “chelate effect” is that it is a result of a different number of water molecules “released” from the first coordination sphere as shown in eq 2



In general, it is not possible to determine the stoichiometric coefficients x , y , and z , experimentally, and Schwarzenbach² therefore suggested a quantitative measure of the chelate effect based on the equilibrium constants $\log \beta_2$ and $\log K_{\text{chel}}$, for the following reactions, where charges have been omitted for simplicity



and



The “chelate effect” is defined as

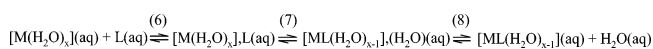
$$\text{Chelate effect} = \log K_{\text{chel}} - \log \beta_2 \quad (5)$$

In the above equations, L is a monodentate and “chel” a bidentate ligand ($L\cap L$) containing the same donor atoms. The origin of the chelate effect has been extensively discussed not only in the literature on the thermodynamics of metal chelate formation,^{4,5} but also in other areas of chemistry. Chelate effects have been invoked as explanation for the rate acceleration in enzyme reactions⁶ and in discussions of molecular association/dissociation in biochemical reactions such as oligomerization, drug–receptor and enzyme–substrate interactions.⁷ The analysis of the thermodynamics of these reactions in aqueous solution is focused on the entropy changes, in which estimates of the translation and rotational contributions play an important role.^{6–8} We will come back to this in the discussion.

Model Reactions and Computational Details

Thermodynamic Model. The new feature in the proposed model is to focus the quantum chemical description on the characteristic chemical event in the reactions, the intramolecular site exchange between water in the first, and a ligand in the second coordination sphere. In the model proposed, denoted Model A, we have divided the stoichiometric complex formation reaction 2 into three parts, in such a way that the equilibrium constants for each step can be accurately

Scheme 1



estimated. Scheme 1, where charges have been omitted for simplicity, shows how this is achieved

The chemical symbols outside the square parenthesis denote species in the second coordination sphere; (aq) denotes the solvent outside the second coordination sphere; steps 6 and 7 are thermodynamic analogues of the Eigen–Wilkins mechanism. The second coordination sphere is thus described using one or more discrete water molecules while the remaining part is described by the continuum model. Reaction 6 has been described using an electrostatic continuum model, the Fuoss equation,^{9a,b} and reaction 7, the intramolecular ligand exchange between the first and second coordination spheres using quantum chemical methods. We have assumed that the Gibbs energy of reaction for eq 8 is zero, that is the complex $[ML(\text{H}_2\text{O})_{x-1}](\text{H}_2\text{O})$ in the solvent is a proper model for $ML(\text{aq})$. The same model can be used for ligand exchange reactions that do not involve the solvent, but in this case the equilibrium constant for reaction 8 must also be estimated using the Fuoss equation, cf. ref 10.

The reactants in our model systems are protolytes, and this may result in proton transfer from the acid (coordinated water) to the base (the carboxylate group); an example is the complex $[\text{UO}_2(\text{oxalate-uni})(\text{H}_2\text{O})_4]$ that forms $[\text{UO}_2(\text{OCO}-\text{COOH})(\text{OH})(\text{H}_2\text{O})_3]$ in gas phase, cf. Fig. S1. This reaction can be avoided by adding water molecules in the second coordination sphere, or by using the CPCM model. However, in the latter case it is not possible to obtain the accurate vibration frequencies necessary to calculate the thermodynamic functions.

The starting structures of the precursor complexes $[M(\text{H}_2\text{O})_x]L$ were generated using the known coordination geometry and by placing the ligand L hydrogen bonded to the exchanging water molecule. In the successor complex $[ML(\text{H}_2\text{O})_{x-1}](\text{H}_2\text{O})$, the outer-sphere water molecule is hydrogen bonded to the ligand L and one of its adjacent water molecules in the first sphere. Several different outer-sphere geometries involving different hydrogen bonding and different number of second sphere water molecules were tested, cf. Table 2.

Computational Details. Molecular structures and electronic energies for all molecules discussed here were calculated following the path of previous studies by our group (see ref 11 and references therein) using the *Gaussian 98* package.¹² We used small core Relativistic Effective Core Potentials for uranium^{13a} and zinc^{13b} centers, and for all second row atoms^{13c} with the corresponding basis sets. We added a set of two polarizing f functions to the zinc basis set with exponents 6.15 and 1.65.^{13d} The basis set of the second row atoms was supplemented with one diffuse p function with exponents 0.04041, 0.05611, 0.0702 for

- (1) Calvin, M.; Bailes, R. H. *J. Am. Chem. Soc.* **1946**, *68*, 949.
- (2) Schwarzenbach, G. *Helv. Chim. Acta* **1952**, *291*, 2344.
- (3) Adamson, A. W. *J. Am. Chem. Soc.* **1954**, *76*, 1578.
- (4) (a) Chung, C.-S. *Inorg. Chem.* **1979**, *18*, 1321. (b) Myers, R. T. *Inorg. Chem.* **1978**, *17*, 952.
- (5) (a) Hancock, R. D.; Martell, A. E. *Comments Inorg. Chem.* **1988**, *6*, 237. (b) Martell, A. E.; Hancock, R. D.; Motekaitis, R. J. *Coord. Chem. Rev.* **1994**, *133*, 39.
- (6) (a) Page, M. I.; Jencks, W. P. *Proc. Natl. Acad. Sci. U.S.A.* **1971**, *68*, 1678. (b) Jencks, W. P. *Proc. Natl. Acad. Sci. U.S.A.* **1981**, *78*, 4046.
- (7) Yu, Y. B.; Privalov, P. L.; Hodges, R. S. *Biophys. J.* **2001**, *81*, 1632.
- (8) Holtzer, A. *Biopolymers* **1995**, *35*, 595.

- (9) (a) Fuoss, R. M. *J. Am. Chem. Soc.* **1958**, *80*, 5059. (b) Morel, F. M. M.; Hering, J. G. *Principles and Applications of Aquatic Chemistry*; John Wiley & Sons Ltd.: New York 1983; p. 399.
- (10) Toraiishi, T.; Privalov, T.; Schimmelpfennig, B.; Wahlgren, U.; Grenthe, I. *J. Phys. Chem. A* **2003**, *107*, 9456.
- (11) Vallet, V.; Moll, H.; Wahlgren, U.; Szabó, Z.; Grenthe, I. *Inorg. Chem.* **2003**, *42*, 1982.
- (12) Frisch, M. J.; Trucks, G. W.; Schlegel, H. B.; Scuseria, G. E.; Robb, M. A.; Cheeseman, J. R.; Zakrzewski, V. G.; Montgomery, J. A., Jr.; Stratmann, R. E.; Burant, J. C.; Dapprich, S.; Millam, J. M.; Daniels, A. D.; Kudin, K. N.; Strain, M. C.; Farkas, O.; Tomasi, J.; Barone, V.; Cossi, M.; Cammi, R.; Mennucci, B.; Pomelli, C.; Adamo, C.; Clifford, S.; Ochterski, J.; Petersson, G. A.; Ayala, P. Y.; Cui, Q.; Morokuma, K.; Malick, D. K.; Rabuck, A. D.; Raghavachari, K.; Foresman, J. B.; Cioslowski, J.; Ortiz, J. V.; Stefanov, B. B.; Liu, G.; Liashenko, A.; Piskorz, P.; Komaromi, I.; Gomperts, R.; Martin, R. L.; Fox, D. J.; Keith, T.; Al-Laham, M. A.; Peng, C. Y.; Nanayakkara, A.; Gonzalez, C.; Challacombe, M.; Gill, P. M. W.; Johnson, B. G.; Chen, W.; Wong, M. W.; Andres, J. L.; Head-Gordon, M.; Replogle, E. S.; Pople, J. A. *Gaussian 98*, revision A.11; Gaussian, Inc.: Pittsburgh, PA, 1998.
- (13) (a) Küchle, W.; Dolg, M.; Stoll, H.; Preuss, H. *J. Chem. Phys.* **1994**, *100*, 7535. (b) Dolg, M.; Wedig, U.; Stoll, H.; Preuss, H. *J. Chem. Phys.* **1987**, *86*, 866. (c) Bergner, A.; Dolg, M.; Küchle, W.; Stoll, H.; Preuss, H. *Mol. Phys.* **1993**, *80*, 1431. (d) Kaupp, M.; Dolg, M.; Stoll, H.; von Schnering, H. G. *Inorg. Chem.* **1994**, *33*, 2122. (e) Woon, D. E.; Dunning, T. H., Jr. *J. Chem. Phys.* **1995**, *103*, 4572. (f) Huzinaga, S. *J. Chem. Phys.* **1965**, *42*, 1293.

Table 1. Thermodynamic Data^a at 298.15 K for the Complex Formation Reaction of Zinc Complexes at Zero Ionic Strength (the corresponding reactions are given in the main text)^b

ligand	entropy change in the gas phase (J/K·mol)				thermodynamics in the gas phase (kJ/mol)			thermodynamics in the solvent (kJ/mol)				
	$\Delta_r S^\circ_{\text{trans}}$	$\Delta_r S^\circ_{\text{rot}}$	$\Delta_r S^\circ_{\text{vib}}$	$\Delta_r S^\circ_{\text{tot}}$	$\Delta_r E$	$\Delta_r H^\circ$	$\Delta_r G^\circ$	$\Delta_r E$	$\Delta_r H^\circ$	$\Delta_r G^\circ$	$\Delta_r G^\circ(7-9)^c$	
model B												
NH ₃	0.6	-4.1	16.9	13.4	-40.5	-38.1	-42.1	-39.6	-37.1	-41.2		
				(9.6)					(-10)	(-13.1)		
2*NH ₃	1.3	-8.1	24.6	17.8	-78.4	-73.7	-79.0	-78.1	-73.4	-78.7		
				(14)					(-23)	(-28.1)		
ethylenediamine (en)	131.4	-11.0	-35.9	84.5	-108.4	-110.1	-135.3	-92.4	-94.1	-119.3		
				(16)					(-30)	(-34.7)		
2*CH ₃ NH ^b	-11.8	-69.3	61.9	-19.9	-116.1	-112.0	-106.0	-77.2	-73.0	-67.1		
model A												
NH ₃	0.0	-0.3	-20.8	21.1	-28.4	-25.3	-19.1	-29.0	-25.9	-19.6	-16.6	
				(9.6)					(-10)	(-13.1)		
2*NH ₃	0.0	-20.9	-17.1	-38.0	-40.7	-35.9	-26.8	-42.4	-37.6	-28.5	-25.5	
									(-23)	(-34.7)		
en-uni ^d	0.0	-0.1	32.1	32.0	-20.6	-18.9	-28.4	-14.5	-12.8	-22.3	-19.3	
en ^d	0.0	-0.2	27.8	27.6	-73.7	-70.1	-78.3	-49.3	-45.7	-53.9	-50.9	
chelate-closure [Zn(en-uni)(H ₂ O) ₅] ²⁺ , (H ₂ O) _m → [Zn(en)(H ₂ O) ₄] ²⁺ , (H ₂ O) _{m+1}												
m = 0	0.0	0.2	3.8	4.1	-47.8	-45.8	-47.0	-34.3	-32.3	-33.6	-	
m = 1	0.0	-0.1	-4.3	-4.4	-53.1	-51.2	-49.9	-34.8	-32.9	-31.6	-	

^a $\Delta_r E$ is the electronic energy at the HF/MP2 level; $\Delta_r S^\circ$, $\Delta_r H^\circ$, and $\Delta_r G^\circ$ are the entropy, enthalpy and Gibbs energy of reaction at 298.15 K, calculated using thermal functions from gas-phase data. ^b The experimental values taken from ref 19 are given within parentheses and refer to a medium with ionic strength 2 M. ^c $\Delta_r G^\circ(7-9)$ is the calculated Gibbs free energy for the total reaction involving eqs 7–9, using the calculated $\Delta_r G^\circ$ value for reaction 8 and the value 0.3 ($\Delta_r G^\circ = 3$ kJ/mol) for the outer-sphere equilibrium constants for reaction 7. See text for further details. ^d In the precursor [Zn(H₂O)₆]²⁺, (en) ethylenediamine is hydrogen bonded to two water molecules located in the first coordination sphere.

Table 2. Thermodynamic Data^a at 298.15 K for the Inner-Sphere Reaction [Zn(H₂O)₆]²⁺, (NH₃)(H₂O)_m → [Zn(NH₃)(H₂O)₅]²⁺, (H₂O)_{m+1}, m = 0, 2, and 5^b

	entropy change in the gas phase (J/K·mol)				thermodynamics in gas phase (kJ/mol)			thermodynamics in the solvent (kJ/mol)			
	$\Delta_r S^\circ_{\text{trans}}$	$\Delta_r S^\circ_{\text{rot}}$	$\Delta_r S^\circ_{\text{vib}}$	$\Delta_r S^\circ_{\text{tot}}$	$\Delta_r E$	$\Delta_r H^\circ$	$\Delta_r G^\circ$	$\Delta_r E$	$\Delta_r H^\circ$	$\Delta_r G^\circ$	$\Delta_r G^\circ(7-9)^c$
experimental data				9.6						-10	-13.1
m = 0											
isomer 1	0.0	-0.3	-20.8	-21.1	-28.4	-25.3	-19.1	-29.0	-25.9	-19.6	-16.6
isomer 2 (cis)	0.0	-0.5	-20.8	-21.4	-29.5	-26.0	-19.6	-33.0	-29.6	-23.2	-20.2
isomer 3 (trans)	0.0	-0.5	-6.2	-6.7	-26.4	-23.2	-21.2	-29.7	-26.5	-24.5	-21.5
m = 2	0.0	0.0	0.0	0.0	-14.8	-13.1	-13.1	-21.7	-20.0	-20.0	-17.0
m = 5	0.0	0.1	12.7	12.8	-20.7	-19.4	-23.2	-19.1	-17.8	-21.7	-18.6

^a $\Delta_r E$ is the electronic energy at the HF/MP2 level; $\Delta_r S^\circ$, $\Delta_r H^\circ$, and $\Delta_r G^\circ$ are the entropy, enthalpy and Gibbs energy of reaction at 298.15 K, calculated using thermal functions from gas-phase data. ^b For m = 0 there are data for three different isomers of [Zn(NH₃)(H₂O)₅]²⁺, (H₂O), with different hydrogen bonding in the second coordination sphere. The experimental values taken from ref 19 refer to a medium with ionic strength 2 M. ^c $\Delta_r G^\circ(7-9)$ is the calculated Gibbs free energy for the total reaction involving eqs 7–9, using the calculated $\Delta_r G^\circ$ value for reaction 8 and the value 0.3 ($\Delta_r G^\circ = 3$ kJ/mol) for the outer-sphere equilibrium constants for reaction 7. See text for further details.

C, ¹³C, ¹³N, ¹³O, and ¹³C respectively, and one polarizing *d* function with exponent 1.0. Hydrogen is described by the parameters suggested by Huzinaga^{13f} with 5*s* functions contracted to 3*s*, supplemented with one polarizing *p* function with the exponent 0.8. We checked the quality of these basis sets by computing the basis set superposition errors (BSSE) on the zinc amine complexes using the counterpoise method of Boys and Bernardi.¹⁴ We split the system in two fragments, [Zn(H₂O)₅]²⁺ and the ligand L, and computed the difference between the energy of the isolated fragments and the energy of the fragments in the complex [Zn(H₂O)₅L]²⁺. The resulting error was always small, less than 4 kJ/mol. Optimal structures were calculated at the Hartree–Fock (HF) level in the gas phase without imposing symmetry constraints. Electron correlation effects were then obtained by single-point MP2 calculations. Solvent effects were accounted for using the CPCM model as implemented in Gaussian 98, again at the optimal gas-phase geometries. The molar entropy, enthalpy, and Gibbs energy of reaction at 25 °C and a pressure of 1 atm. were calculated at the gas-phase geometry using standard statistical mechanics formulas.¹⁵ It was necessary to calculate the energy levels in the gas phase because the Gaussian 98 version used does not allow computation of analytical second derivatives with the solvent model. The translation and rotation entropy contributions were calculated from the mass and the moments

of inertia of the molecule taking its symmetry into account. A special problem arises for molecules with functional groups such as the CH₃ group in methylamine and coordinated water that can have “internal” rotations; one of the vibrational degrees of freedom of the molecule will then be associated with an oscillation about the bond joining the two groups. These modes are described as low-frequency harmonic oscillators in the default version of most quantum chemical packages. Because harmonic oscillation and free rotation have quite different partition functions,¹⁶ the harmonic oscillator treatment of internal rotations may lead to errors in the entropy estimate. However, the error in the total entropy is fairly small at room temperature¹⁷ as indicated in Table 5, cf. Discussion. For small molecules, the hindered rotor option of Gaussian 98 made it possible to identify the internal rotation modes and treat them using the procedure defined by Ayala and Schlegel.¹⁶ The method was tested against experimental data for methylamine and ethylenediamine, as discussed in the Results section. For the large complexes discussed here it was not possible to identify the internal rotation modes in this way. This is a minor problem, as one may expect them to be highly restricted due to hydrogen bond interactions with the solvent, and thus execute vibrational motion at room temperature. For this reason, we have calculated all gas-phase entropies assuming that internal rotations are absent and that all

(14) Boys, S. F.; Bernardi, F. *Mol. Phys.* **1970**, *19*, 553.(15) Pitzer, K. S. *Thermodynamics*; MacGraw-Hill: New York, 1961.(16) Ayala, P. Y.; Schlegel, H. B. *J. Chem. Phys.* **1998**, *108*, 2314.(17) Katzer, G.; Sax, A. F. *J. Phys. Chem. A.* **2002**, *106*, 7204.

Table 3. Thermodynamic Data at 298.15 K and Zero Ionic Strength for Reactions in the Binary UO_2^{2+} –Oxalate System^a

reaction	reaction N ^o	entropy change (J/K·mol)			thermodynamics in gas phase (kJ/mol)			thermodynamics in solvent (kJ/mol)		
		$\Delta_r S_{\text{rot}}^{\circ}$	$\Delta_r S_{\text{vib}}^{\circ}$	$\Delta_r S_{\text{tot}}^{\circ}$	$\Delta_r E$	$\Delta_r H^{\circ}$	$\Delta_r G^{\circ}$	$\Delta_r E$	$\Delta_r H^{\circ}$	$\Delta_r G^{\circ}$
$[\text{UO}_2(\text{H}_2\text{O})_5]^{2+} + (\text{oxalate})^{2-} \rightleftharpoons [\text{UO}_2(\text{oxalate})(\text{H}_2\text{O})_3] + 2\text{H}_2\text{O}$	(13)	−3.6	−34.4	88.7 ^b	−1650	−1657	−1683	−87.2	−94.3	−120.7
$[\text{UO}_2(\text{oxalate})(\text{H}_2\text{O})_3] + (\text{oxalate})^{2-} \rightleftharpoons [\text{UO}_2(\text{oxalate})_2(\text{H}_2\text{O})]^{2-} + 2\text{H}_2\text{O}$	(14)	−4.0	5.7	128.2 ^c	−487.9	−495.8	−534.6	−104.8	−112.6	−150.8 (−24.7)
chelate ring closure with constant coordination number										
$[\text{UO}_2(\text{oxalate-uni})(\text{H}_2\text{O})_4] \cdot (\text{H}_2\text{O}) \rightleftharpoons [\text{UO}_2(\text{oxalate})(\text{H}_2\text{O})_3] \cdot (\text{H}_2\text{O})_2$	(15)	0.7	20.7	21.4	−107.8	−118.2	−107.5	−29.6	−26.9	−33.3
$[\text{UO}_2(\text{oxalate})(\text{oxalate-uni})(\text{H}_2\text{O})_2]^{2-} \rightleftharpoons [\text{UO}_2(\text{oxalate})_2(\text{H}_2\text{O})]^{2-} \cdot (\text{H}_2\text{O})$	(16)	1.2	41.1	42.3	−33.9	−34.3	−46.9	−4.9	−5.3	−17.9
$[\text{UO}_2(\text{oxalate})(\text{oxalate-uni})_2(\text{H}_2\text{O})]^{4-} \rightleftharpoons [\text{UO}_2(\text{oxalate})_2(\text{oxalate-uni})]^{4-} \cdot (\text{H}_2\text{O})$	(17)	−0.6	28.0	27.5	−7.9	−8.9	−17.1	−4.0	−5.0	−14.5
$[\text{UO}_2(\text{oxalate})(\text{oxalate-uni})(\text{H}_2\text{O})]^{2-} \rightleftharpoons [\text{UO}_2(\text{oxalate})_2]^{2-} \cdot (\text{H}_2\text{O})$	(18)	0.5	13.3	13.8	−58.4	−57.2	−61.3	0.5	1.7	−2.4
chelate ring closure with increase in the coordination number										
$[\text{UO}_2(\text{oxalate})(\text{carbox})(\text{oxalate-uni})]^{4-} \rightleftharpoons [\text{UO}_2(\text{oxalate})_2(\text{carbox})]^{4-}$	(19)	−1.3	−5.7	−7.0	39.7	40.8	42.8	−18.2	−17.5	−15.4
$[\text{UO}_2(\text{oxalate})(\text{oxalate-uni})_2]^{4-} \rightleftharpoons [\text{UO}_2(\text{oxalate})_2(\text{oxalate-uni})]^{4-}$	(20)	−1.4	−25.4	−26.8	−16.3	−15.9	−7.9	−78.7	−78.3	−70.3
$[\text{UO}_2(\text{oxalate})(\text{oxalate-uni})(\text{H}_2\text{O})]^{2-} \rightleftharpoons [\text{UO}_2(\text{oxalate})_2(\text{H}_2\text{O})]^{2-}$	(21)	−1.4	−6.1	−7.5	−94.3	−92.4	−90.1	−84.8	−82.9	−80.7
chelate ring closure at the carboxylate end										
$[\text{UO}_2(\text{oxalate})_2(\text{oxalate-uni})]^{4-} \rightleftharpoons [\text{UO}_2(\text{oxalate})_2(\text{carbox})]^{4-}$	(22)	−0.5	−1.0	−1.5	35.0	35.7	36.2	14.0	14.8	15.2
$[\text{UO}_2(\text{oxalate})(\text{carbox})(\text{oxalate-uni})]^{4-} \rightleftharpoons [\text{UO}_2(\text{oxalate})(\text{carbox})_2]^{4-}$	(23)	−0.5	−6.4	−7.0	39.7	40.3	42.4	−17.5	−16.9	−14.8
$[\text{UO}_2(\text{oxalate})(\text{oxalate-uni})_2]^{4-} \rightleftharpoons [\text{UO}_2(\text{oxalate})(\text{carbox})(\text{oxalate-uni})]^{4-}$	(24)	−0.6	−20.6	−21.6	−21.0	−20.5	−14.2	−46.5	−46.0	−39.7
$[\text{UO}_2(\text{oxalate})(\text{oxalate-uni})(\text{H}_2\text{O})]^{2-} \rightleftharpoons [\text{UO}_2(\text{oxalate})(\text{carbox})(\text{H}_2\text{O})]^{2-}$	(25)	−0.8	−2.1	−3.0	−25.4	−23.4	−22.5	−35.0	−33.3	−32.4

^a Reactions 13 and 14 are chelate ring closure involving both carboxylate groups; reactions 15–18 are chelate ring closure reactions with retained coordination number, reactions 19–21 take place with an increase from four to five coordination. Reactions 22–25 involve chelate ring closure reaction at one carboxylate end. The experimental values taken from ref 23c are given within parentheses and refer to extrapolated values at zero ionic strength. ^b The translational contribution to the entropy change $\Delta_r S_{\text{trans}}^{\circ}$ is 126.7 J/K·mol. ^c The translational contribution to the entropy change $\Delta_r S_{\text{trans}}^{\circ}$ is 126.5 J/K·mol.

Table 4. Thermodynamic Data at 298.15 K and Zero Ionic Strength for the Chelate Ring Closure Reactions in the Ternary UO_2^{2+} –Oxalate–Fluoride System

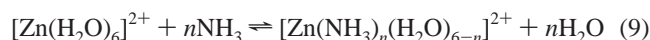
reaction	reaction N ^o	entropy change (J/K·mol)			thermodynamics in gas phase (kJ/mol)			thermodynamics in solvent (kJ/mol)		
		$\Delta_r S_{\text{rot}}^{\circ}$	$\Delta_r S_{\text{vib}}^{\circ}$	$\Delta_r S_{\text{tot}}^{\circ}$	$\Delta_r E$	$\Delta_r H^{\circ}$	$\Delta_r G^{\circ}$	$\Delta_r E$	$\Delta_r H^{\circ}$	$\Delta_r G^{\circ}$
chelate ring closure with increase in the coordination number										
$[\text{UO}_2(\text{oxalate})(\text{oxalate-uni})\text{F}]^{3-} \rightleftharpoons [\text{UO}_2(\text{oxalate})_2\text{F}]^{3-}$	(26)	−7.4	−43.8	−51.1	−43.6	−43.2	−27.9	−82.9	−82.4	−67.2
$[\text{UO}_2(\text{oxalate-uni})\text{F}_3]^{3-} \rightleftharpoons [\text{UO}_2(\text{oxalate})\text{F}_3]^{3-}$	(27)	−8.0	−26.3	−34.3	11.5	11.8	22.1	−47.4	−47.0	−36.8
$[\text{UO}_2(\text{oxalate-uni})\text{F}_3]^{3-} \cdot (\text{H}_2\text{O}) \rightleftharpoons [\text{UO}_2(\text{oxalate})\text{F}_3]^{3-} \cdot (\text{H}_2\text{O})$	(28)	−1.7	−17.6	−19.3	−0.4	−0.7	5.0	−44.3	−44.5	−38.8
chelate ring closure at the carboxylate end										
$[\text{UO}_2(\text{oxalate})(\text{oxalate-uni})\text{F}]^{3-} \rightleftharpoons [\text{UO}_2(\text{oxalate})(\text{carbox})\text{F}]^{3-}$	(29)	−0.8	−38.0	−38.8	−32.7	−32.2	−20.7	−52.8	−52.4	−40.8
$[\text{UO}_2(\text{oxalate-uni})\text{F}_3]^{3-} \rightleftharpoons [\text{UO}_2(\text{carbox})\text{F}_3]^{3-}$	(30)	−1.3	−20.2	−21.5	−1.8	−1.4	5.0	−31.9	−31.5	−25.1

vibrations are harmonic. Following the argument of Tomasi and Persico,¹⁸ we assume the vibrations to be the same in a vacuum and in solution.

Results

Structure and Thermodynamics of the Zn(II)–Ammonia and Methylamine Systems. The geometry and the thermodynamic functions of the complexes $[\text{Zn}(\text{H}_2\text{O})_6]^{2+}$; $[\text{Zn}(\text{H}_2\text{O})_6]^{2+}$, (NH_3) ; $[\text{Zn}(\text{H}_2\text{O})_6]^{2+}$, $(\text{NH}_3)(\text{H}_2\text{O})_m$, $[\text{Zn}(\text{NH}_3)(\text{H}_2\text{O})_5]^{2+}$, $(\text{H}_2\text{O})_{m+1}$,

both with $m = 0, 2, 5$; cis- and trans- $[\text{Zn}(\text{H}_2\text{O})_6]^{2+}$, $(\text{NH}_3)_2$; $[\text{Zn}(\text{NH}_3)_2(\text{H}_2\text{O})_4]^{2+}$, $(\text{H}_2\text{O})_2$; cis- $[\text{Zn}(\text{CH}_3\text{NH}_2)_2(\text{H}_2\text{O})_4]^{2+}$ and the corresponding species omitting ligands in the second coordination sphere are given in Figures 1, S2, and S3, Tables 1, 2, S1, S2, and S3. These data allow us to compare the thermodynamics calculated using model A with model B and with experimental data. In model B, the Gibbs energy of reaction for



is calculated in the solvent using the thermodynamic functions

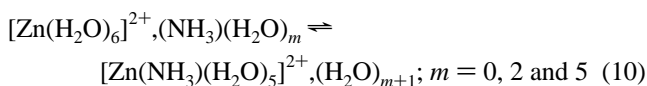
(18) Tomasi, J.; Persico, M. *Chem. Rev.* **1994**, *94*, 2027.

Table 5. Calculated (Hartree–Fock) and Experimental Entropy Data in J/mol·K of the Gaseous Methylamine and Ethylenediamine Ligands and of the Complexes $[\text{Zn}(\text{CH}_3\text{NH}_2)_2(\text{H}_2\text{O})_4]^{2+}$ and $[\text{Zn}(\text{en})(\text{H}_2\text{O})_4]^{2+}$ at 298.15 K and 1 Atm

entropy contribution	methylamine		ethylenediamine		$[\text{Zn}(\text{CH}_3\text{NH}_2)_2(\text{H}_2\text{O})_4]^{2+}$	$[\text{Zn}(\text{en})(\text{H}_2\text{O})_4]^{2+}$	$\frac{S([\text{Zn}(\text{en})(\text{H}_2\text{O})_4]^{2+})}{S([\text{Zn}(\text{CH}_3\text{NH}_2)_2(\text{H}_2\text{O})_4]^{2+})}$			
	this work		ref 4a				this work	this work	this work	ref 4a
	without internal rotation	with internal rotation	without internal rotation	with internal rotation			data for the corresponding Cd complexes			
translation	151.5	151.5	150.9	159.8	159.8	159.1	174.7	174.6	−0.1	≅ 0
rotation	80.8	80.8	81.1	101.8	101.8	96.4	127.6	126.2	−1.4	≅ −5.9
internal rotation		12.1	7.7	−	40.3	62.3	−	−	−	≅ −43.9
vibration	6.3	1.89	2.3	41.4	10.5	10.6	308.7	243.2	−65.5	≅ −5.9
total	238.7	246.3	242.0	303.0	312.4	328.4	611.0	544.0	−67.0	≅ −53.5

for each reactant and product. The Gibbs energy of reaction for model A, described by eqs 6–8 is obtained by using the value 0.3^{9b} ($\Delta_r G^\circ = 3.0$ kJ/mol) for the outer-sphere equilibrium constant of reaction 6, as estimated from the Fuoss equation and by using the ab initio values for the intramolecular reaction 7. The resulting Gibbs energy of reaction is -16.6 and -25.5 kJ/mol for $n = 1$ (isomer 1) and $n = 2$ (the cis-isomer), respectively, in good agreement with the Gibbs energy of reaction, $\Delta_r G^\circ$, obtained from experimental equilibrium constants, -13.1 and -28.2 kJ/mol, respectively. The Gibbs energy of reaction for the second model described by reaction 9, is -41.2 kJ/mol for $n = 1$ and -78.7 kJ/mol for $n = 2$ (the cis-isomer), cf. Table 1. The difference in electronic energy and entropy between the cis- and trans-isomers of $[\text{Zn}(\text{H}_2\text{O})_4(\text{NH}_3)_2]^{2+}$ is small, less than 2 kJ/mol and 2 J/K·mol, respectively. The experimental values for the corresponding enthalpy of reaction taken from *Critical Stability Constants*^{19a} are -11 and -28 kJ/mol, with estimated errors of at least 2 kJ/mol. These values are about 12 kJ/mol less negative than the enthalpy of reaction for the intramolecular reaction 8, -25.9 and -37.6 kJ/mol for $n = 1$ and 2, respectively. The enthalpy of reaction calculated using reaction 9 is -37.1 and -73.4 kJ/mol for $n = 1$ and 2, respectively. The Zn–water bond distances in the different structures are close to those found by Pavlov et al.,^{20a} Díaz et al.,^{20b} and in crystal structures.^{21,22} The Zn(II)–ammonia distances are also in good agreement with data from crystal structures.²²

Testing of the Intramolecular Thermodynamic Model Using the Zn(II)–Ammonia Complexes. To determine how sensitive the calculated thermodynamic data are for the structure details in the proposed “intramolecular” model, we have studied the reaction



The data given in Table 2 show that the Gibbs energy of reaction is not strongly dependent on the stoichiometry and geometry of the second sphere, even the simplest second sphere

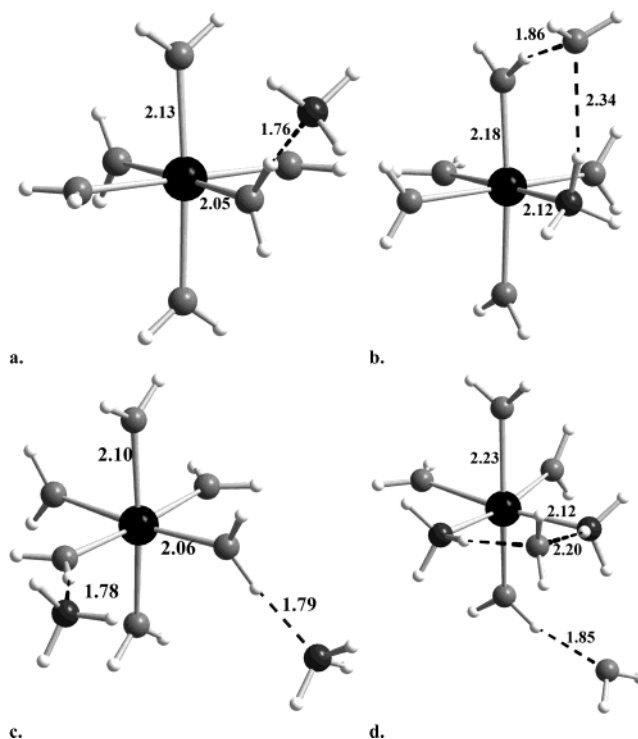


Figure 1. Perspective views of the structures of the complexes (a) $[\text{Zn}(\text{H}_2\text{O})_6]^{2+}, (\text{NH}_3)$; (b) $[\text{Zn}(\text{NH}_3)(\text{H}_2\text{O})_5]^{2+}, (\text{H}_2\text{O})$; (c) $[\text{Zn}(\text{H}_2\text{O})_6]^{2+}, (\text{NH}_3)_2$; and (d) cis- $[\text{Zn}(\text{NH}_3)_2(\text{H}_2\text{O})_4]^{2+}, (\text{H}_2\text{O})_2$. The ligands outside the square brackets are located in the second coordination sphere. The bond distances are average values given in Å; the dashed line indicates hydrogen bond interactions.

model catches the chemical characteristics of the reactions; however, the values of the enthalpy and entropy of reaction for different outer-sphere geometries vary more and in such a way that their contributions to the Gibbs energy of reaction to a large extent compensate one another. The entropy of reaction is negative for the simplest model ($m = 0$) but is positive for the more realistic model ($m = 5$), the latter in agreement with experimental data.

Structure and Thermodynamics of the Zn(II)–Ethylenediamine Complexes. The structure of the complexes $[\text{Zn}(\text{H}_2\text{O})_6]^{2+}, (\text{en})$; $[\text{Zn}(\text{en-uni})(\text{H}_2\text{O})_5]^{2+}, (\text{H}_2\text{O})_m$; $[\text{Zn}(\text{en})(\text{H}_2\text{O})_4]^{2+}, (\text{H}_2\text{O})_{m+1}$, both with $m = 0, 1$; $[\text{Zn}(\text{en})(\text{H}_2\text{O})_4]^{2+}$; where (en-uni) and (en) denote ethylenediamine ($\text{NH}_2\text{CH}_2\text{CH}_2\text{NH}_2$) coordinated to one and two NH_2 -groups, respectively, are given in Figure 2 and as Supporting Information in Tables S1 and S3 and Figures S2 and S4. The electronic energy, entropy, and Gibbs energy and enthalpy of the various Zn(II) complexes are given in Tables 1 and S2.

(19) (a) Smith, R. M.; Martell, A. E. *Critical Stability Constants. Vol 4: Inorganic Complexes*; Plenum Press: New York, 1976. (b) Smith, R. M.; Martell, A. E. *Critical Stability Constants. Volume 6: Second Supplement*; Plenum Press: New York, 1989.

(20) (a) Pavlov, M.; Siegbahn, P. E.; Sandström, M. *J. Phys. Chem. A* **1998**, *102*, 219. (b) Díaz, N.; Suárez, D.; Merz, K. M., Jr. *Chem. Phys. Lett.* **2000**, *326*, 288.

(21) Simmons, C. J.; Hitchman, M. A.; Stratemeier, H. *Inorg. Chem.* **2000**, *39*, 6124.

(22) Wells, A.-F. *Structural Inorganic Chemistry*, Fifth Ed.; Clarendon Press: Oxford 1985; pp. 1151–1156.

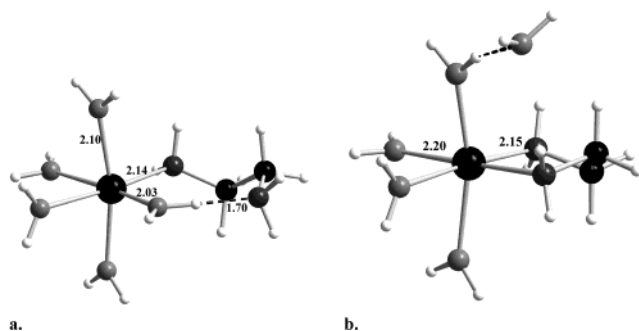


Figure 2. Perspective views of the structures of (a) $[\text{Zn}(\text{en-uni})(\text{H}_2\text{O})_5]^{2+}$ and (b) $[\text{Zn}(\text{en})(\text{H}_2\text{O})_4]^{2+}, (\text{H}_2\text{O})$ complexes, where (en-uni) and (en) denote ethylenediamine coordinated through one and two amino groups, respectively. The bond distances are average values given in Å; the dashed line indicates hydrogen bond interactions.

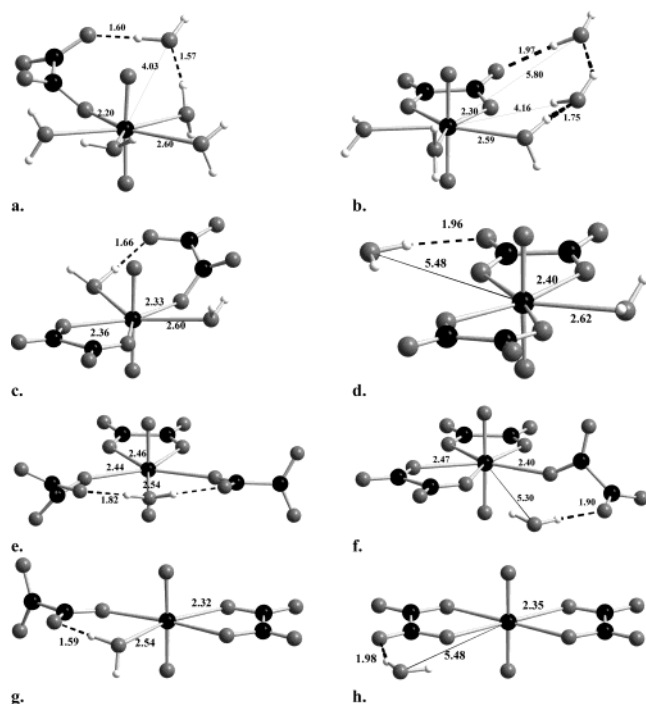
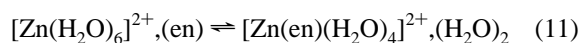


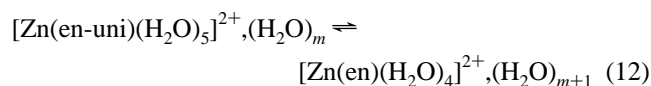
Figure 3. Structures of the reactants and products involved in the oxalate chelate ring closure reactions with constant coordination number, cf. eqs 15–18 in Table 3. The bond distances are average values given in Å; the dashed line indicates hydrogen bond interactions.

The Gibbs energy of reaction for model A



is -50.9 kJ/mol, in fair agreement with the experimental value -34.7 kJ/mol, while that for model B, -119.3 kJ/mol, deviates strongly.

The thermodynamic data for the chelate ring closure reactions



given in Table 1, $\Delta_r G^\circ = -33.6$ and -31.6 kJ/mol for $m = 0$ and 1, respectively, indicate that the structure of the second coordination sphere also in this case has a small influence on the Gibbs energy of reaction. The experimental value of the Gibbs energy of reaction for the formation of the $\text{Zn}(\text{en-uni})$ is not known; however the calculated value -19.3 kJ/mol is close

to that for the ammonia complex, -13.1 kJ/mol, as one might expect for chemical reasons.

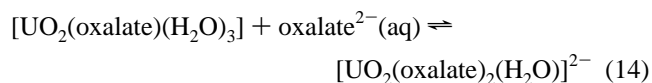
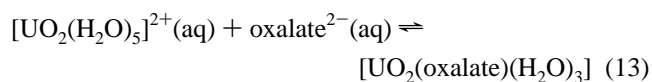
The enthalpy term gives the main contribution to the Gibbs energy of reaction in both solvent and gas phase, this is consistent with experimental observations on other amine systems (Cu, Ni, and Cd).^{5b, Table 3, 22b}

The change in entropy for chelate ring closure is close to zero, 4.1 J/K·mol, for the Zn–ethylenediamine system.

The translation entropy contribution is very small in the reactions where the number of reactants and products is the same. It is apparent from the data in Tables 1 and 3 that vibration and rotation entropy contributions are significant in all systems.

Structure and Thermodynamics of the Binary and Ternary Uranyl(VI)–Oxalate Complexes. When studying the “intramolecular” model for the U(VI)–oxalate systems, we found that complexes with oxalate in the second coordination sphere were not stable, a proton was transferred from coordinated water to oxalate. In the gas phase, this could be avoided by adding several water molecules in the second coordination sphere. As this made the calculations very time-consuming, we decided to restrict the investigation to the thermodynamics of chelate ring closure reactions, starting with structures with a unidentate oxalate. In this way, we could use data on the structure and thermodynamic functions for the isomers of $[\text{UO}_2(\text{oxalate})_3]^{4-}$, $[\text{UO}_2(\text{oxalate})_2(\text{H}_2\text{O})]^{2-}$, $[\text{UO}_2(\text{oxalate})\text{F}_3]^{3-}$, and $[\text{UO}_2(\text{oxalate})_2\text{F}]^-$ reported in one of our previous publications.¹¹ In the present study, we have added some new data on the five-coordinated isomers for the mono-, bis-, and tris-oxalate complexes. Geometries of the complexes optimized in the present study are given in Table S4 and in Figures 3 and S5. The coordinates are reported in Tables S7.

The Gibbs energy of reaction for the formation of $\text{UO}_2(\text{oxalate})(\text{H}_2\text{O})_3$ and $[\text{UO}_2(\text{oxalate})_2(\text{H}_2\text{O})]^{2-}$ defined by



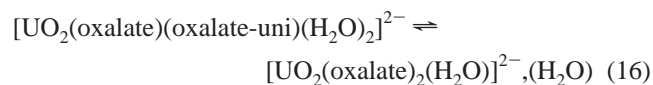
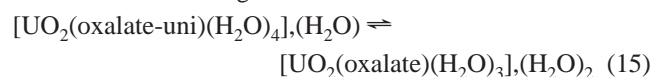
are -120.7 kJ/mol, -150.8 kJ/mol, respectively, cf. Table 3. These values differ significantly from the experimental ones for the formation of $\text{UO}_2(\text{oxalate})(\text{aq})$ and $\text{UO}_2(\text{oxalate})_2^{2-}(\text{aq})$, -42.1 and -24.7 kJ/mol.^{23c} As observed for the Zinc complexes, large errors are made when calculating thermodynamics quantities from model B. An estimate of the Gibbs energy of reaction for the “intramolecular” model can be obtained from the thermodynamics of the chelate ring opening/ring closure reactions. We have investigated different ring closure reactions: The first, reactions 15–18 in Table 3, with retained coordination number in the equatorial plane of the uranyl unit, require that we include one or two hydrogen bonded water molecules in the second coordination sphere. The second takes place with an increase in coordination number from five to six, reaction 19, or from four to five, reactions 20 and 21. In these equations (oxalate-uni) and (oxalate) denote oxalate coordinated

(23) (a) Havel, J. *Collect. Czech. Chem. Commun.* **1969**, *34*, 3248. (b) Havel, J.; Soto-Guerrero, J.; Lubal, P. *Polyhedron* **2002**, *21*, 1411. (c) Ferri, D.; Iuliano, M.; Manfredi, C.; Vasca, E.; Curaso, T.; Clemente, M.; Fontanella, C. *J. Chem. Soc., Dalton Trans.* **2000**, 3460.

to a single carboxylate oxygen and chelate bonded oxalate, respectively. In the third set of reactions the chelate ring closure takes place at the same carboxylate group, resulting in the formation of a four-member ring, denoted (carbox). This results in an increase of the equatorial coordination number from five to six in reactions 22 and 23, and from four to five in reactions 24 and 25.

For the ternary complexes, we have used the structures reported in ref 11 to determine the thermodynamics of ring closure reactions involving both carboxylate ends (reactions 26–28) and at a single carboxylate end (reactions 29 and 30), cf. Table 4; all of which result in an increase in the coordination number from four to five. The electronic energies and thermodynamics quantities for the binary and ternary complexes are given in Table S5–S6. The U–water and U–O_{ox} bond distances in the bis-oxalate and tris-oxalate compounds are close to those found in other isomers.¹¹ However, in [UO₂(oxalate-uni)-(H₂O)₄],(H₂O) and [UO₂(oxalate)(H₂O)₃],(H₂O)₂ the U–O_{ox} distances are significantly shorter, 2.20 and 2.30 Å for the unidentate and the chelating oxalate, respectively.

To be consistent with the experimental data, the Gibbs energy of reaction for the ring closure reactions



must be smaller in absolute value (less negative) than the experimental values for the reactions 13 and 14. This is indeed the case for this intramolecular reaction, as shown by the calculated values for reactions 15 and 16, –33.3, and –17.9 kJ/mol, respectively. There are no experimental data for the ring closure reactions 15 and 16. The experimental enthalpy of reaction for 13 is about 10 kJ/mol, estimated from the corresponding uranyl(VI)–malonate system;^{22a,24} this is reasonably close to the enthalpy of reaction, –5 kJ/mol, for the chelate ring closure reactions 16, 17, and 18, cf. Table 3. The entropy change for the chelate ring closure reactions in the U(VI)–oxalate systems varies between 13.8 and 42.3 J/K·mol when there is no change in the coordination number in the equatorial plane, in other cases the entropy change is negative.

Discussion

Thermodynamic Model. The results described in the previous sections show that the quantum chemical estimation of the Gibbs energy of reaction in solution for two very different metal ions, Zn²⁺ and UO₂²⁺, and different ligands (oxalate and different amines) are in much better agreement with experiment when using the “intramolecular” model A than that obtained using the quantum chemical estimates for each reactant and product (Model B) in the stoichiometric total reaction. Good agreement between the calculated and experimental Gibbs energy of reaction has also been obtained for the reaction



when it is modeled by eqs 6–8 as discussed in a previous study.¹⁰

To calculate accurate thermodynamic data for chemical reactions in aqueous solution using quantum chemical methods, it is necessary to use a model that describes solvation effects in a proper way. There are two important assumptions in the model we have used: (i) that the effect of solvation on the electronic energy of reaction can be described by the CPCM model, and (ii) that the entropy of reaction is the same in gas phase and solution. These assumptions are briefly discussed below.

The magnitude of the solvation energy estimated by the CPCM model depends on the size and charge of the solute. The reactants and products in Model B have very different structures and in the oxalate case different charges; the difference in their solvation properties is therefore much larger than that between the reactant and product complexes in Model A. We thus expect that the solvation contribution to the electronic energy of reaction will be smaller for model A, where the size and charge distribution of reactant and product are more similar than in model B. We have demonstrated that the Gibbs energy of reaction is not strongly dependent on the structure of the second coordination sphere. The changes in the enthalpy and entropy of reaction are somewhat larger between the models with different numbers of water in the second coordination sphere and compensating one another. By using a larger second coordination sphere, the intramolecular model gives results that are close to the experimental values (cf. Table 2). We suggest that the calculated entropy of reaction in the larger model includes part of the solvation entropy, which is important, but not easy to predict. There is a price to pay for the larger model, the computing time is increased by a factor of 4 to 5 as compared to the simplest one.

Entropy Estimates. Calculation of the translation and rotation entropy (excluding “internal” rotations) contributions is straightforward and only depends on the mass and moments of inertia of the species. The computed contributions from vibration and internal rotation modes depend on the accuracy of the calculation; in a previous study we have found good agreement between experimental and calculated vibration energy levels for a number of uranium(VI) compounds in gas phase.²⁵ This observation provides a validation of the method used to calculate the energy levels, but it does not resolve the problem to identify the low-frequency modes that are due to “internal” rotation, except for small molecules such as methylamine and ethylenediamine. We have compared the entropy of these ligands in the gas phase with experimental data discussed by Chung.^{4a} The results reported in Table 5 show a satisfactory agreement between the calculated and experimental data, taking internal rotation into account; the sum of the entropy contribution from vibration and “internal” modes is about 10 J/K·mol larger than the calculated one by considering all modes as harmonic. Because of the restrictions on “internal” modes due to hydrogen bond interactions with the solvent we have treated all the 3*N* – 6 “vibrational” degrees of freedom as harmonic oscillators in the calculation of the entropy changes and expect the errors in the entropy of reaction introduced by this assumption to cancel when using model A. The contribution of symmetry¹⁵ to the entropy –*R*lnσ has to be accounted for in reactions with polyatomic molecules. In gas phase, it is straightforward to identify the symmetry of the structure of lowest energy and to determine

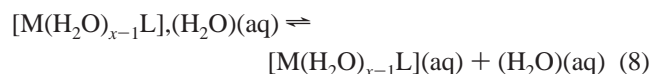
(24) Rao, L.; Jiang, J.; Zanonato, P.; Di Bernardo, P.; Bismondo, A.; Garnov, A. Y. *Radiochim. Acta* **2002**, *90*, 581.

(25) Privalov, T.; Schimmelpfennig, B.; Wahlgren, U.; Grenthe, I. *J. Phys. Chem. A* **2002**, *106*, 11 277.

the symmetry number σ , corresponding to the number of equivalent orientations. For instance, the formation of a chelate ring from unidentate ethylenediamine and oxalate ligands is expected to result in an entropy contribution of $-R\ln 2$ for each chelate ring formed. In the solvent, the geometry of the complexes is likely to differ from the ideal gas-phase structures, and in the absence of symmetry information in solution, we have chosen not to consider symmetry contributions to the thermodynamics quantities, assuming these contributions to cancel. A different approach has been followed by Chung,^{4a} who estimated symmetry effects in the octahedral complexes $[\text{Cd}(\text{CH}_3\text{NH}_2)_2(\text{H}_2\text{O})_4]^{2+}$ and $[\text{Cd}(\text{en})(\text{H}_2\text{O})_4]^{2+}$, assuming free rotation of the methyl group. This results in different vibration and rotation entropy contributions from that obtained in our study, cf. Table 5, last column.

Our model is based on the assumption of equal entropy of reaction in gas phase and solvent, but we do not imply that the standard entropies of reactants and products are the same in the two phases; it is well-known that the entropy of solvation is large,^{4a} e.g., -117.1 and -150.6 J/K·mol, for methylamine and ethylenediamine, respectively. Lucas²⁶ reported that the entropy of solution of gases in water is almost entirely a function of molecular size, as this is very similar in the reactant and product complexes in model A, we expect very similar entropies of solvation in this “intramolecular” model. The entropy of reaction depends on the structure of the second coordination sphere and the model calculations on the Zn(II)–ammonia system indicates that the model with the most detailed description of the second sphere gives a computed entropy of reaction that is closer to the experimental value. However, there are computational limitations on the size of the second sphere, in particular for complexes with very heavy atoms, such as actinides.

The assumption that the change in Gibbs energy for reaction 8 is small receives some support by the computed entropy change for the transfer of water in the second coordination sphere to the bulk



From the data given in Table S8 and the experimental entropy of $\text{H}_2\text{O}(\text{l}, 298.15 \text{ K})$, 70 J/K·mol, we obtain a small average entropy change for the transfer of water from the second coordination sphere to the bulk solvent of 16 J/K·mol for the five coordinated complexes and -12 J/K·mol for the four coordinated $[\text{UO}_2(\text{oxalate})_2]^{2-}$.

The “intramolecular” model A, based on gas-phase entropy estimates provides good estimates of the Gibbs energy of reaction in solution for systems with quite different chemistry; this is probably a result of compensation of errors both in the solvation entropy and in the CPCM model. However, a model requirement is that both the outer-sphere reactant and product are stable species. In this study and in ref 10, we have demonstrated that this is the case for ligands of charge 0 or -1 . The model can also be used for ligands with a larger negative charge, but this requires additional water molecules in the second coordination sphere and a large increase in the computation time.

(26) Lucas, M. *Bull. Soc. Chim. Fr.* **1969**, *64*, 1792.

Thermodynamics of Chelate Ring Closure Reactions and the Chelate Effect. It has been stated, cf. ref 5b p 40, that “Entropy effects are associated with freedom of motion in both the metal ion and the ligand, and consists of translational entropy of the solutes involved as well as the internal forms of entropy such as freedom of vibration and rotation.” The problem with general statements of this type is to quantify them; this cannot be done beginning from macroscopic data. The process requires the microscopic perspective provided by quantum chemistry, as discussed in the following section. The entropy change for reaction 1 is nearly always much larger for multidentate than for monodentate ligands and most discussions of the chelate effect have therefore been focused on the entropy changes in complex formation equilibria. We will begin with the translation entropy. Calvin and Bailes¹ suggested the first “microscopic” interpretation of the chelate effect and described it as a change of translation entropy due to the different number of reactants and products in eq 1. As it is difficult or impossible to measure the change in solvation of reactants and products, Schwarzenbach² introduced an operational definition of the “chelate effect” based on measurable quantities, eq 5. Adamson³ suggested that the entropy effect “disappears” by changing the molar concentration scale to mol fractions; this is equivalent with a change in free volume for the solute resulting in a change of translation entropy. The relationship between the entropy of reaction on the mol fraction, ΔS^X , and molar concentration, ΔS^M , scales is given by

$$\Delta S^X = \Delta S^M - \Delta n R \ln(1000 \rho_1 / M_1) \approx \Delta S^M - \Delta n R \ln 55.5 \quad (32)$$

where Δn is the difference between the sum of the stoichiometric coefficients for products and reactants in the chemical reaction discussed, ρ_1 and M_1 are the density and mol weight of the solvent, water in this case. The last term in eq 32, the so-called cratic entropy term, has been used to estimate translation entropy contributions in other chemical reactions.^{6,7,27} The thermodynamic and statistical mechanics basis for this has been thoroughly discussed by Holtzer,⁸ who concludes “Although removal of translational effects is useful in interpreting free energy and entropy changes in molecular terms, this particular correction (the cratic entropy term) does not do so. ... We find no justification ... for the primacy of mole fraction concentration units for solute in ideal dilute solutions”. To this can be added that the experimental manifestations of the “chelate effect” do not “disappear” by a change of concentration units, cf. ref 28. Holtzer⁸ also points out that the concept “translation” is ambiguous when applied to reactions in solution. The quantum chemical results provide more detailed information of the entropy contributions in the chemical reactions studied here, including the chelate effect. The data in Table 1 show that the (gas phase) translation entropy contribution to the entropy of reaction can be significant, but that rotation and vibration entropy contributions are at least as important. They also show that the entropy change is not related to the “cratic” entropy

(27) (a) Searle, M. S.; Williams, D. H. *J. Am. Chem. Soc.* **1992**, *114*, 10 690. (b) Searle, M. S.; Williams, D. H.; Gerhard, U. *J. Am. Chem. Soc.* **1992**, *114*, 10 697.

(28) Siemeling, U.; Türk, T.; Schoeller, W. W.; Redshaw, C.; Gibson, V. C. *Inorg. Chem.* **1998**, *37*, 4738.

term as suggested by Adamson. The reactions studied here show that the enthalpy of reaction can give a large contribution to the Gibbs free energy of reaction in complex formation reactions, as also indicated by experimental data.^{5,22} It is thus misleading to describe the strong stability of chelate complexes as a translation entropy effect alone.

The analysis of different model reactions demonstrates that the chelate effect is not only due to translation entropy contributions, but also rotation and vibration contributions are at least as important. Important contributions to the entropy term come from low-frequency vibration modes, some of which correspond to internal rotation motions. In solution, we expect that these modes are hindered by interactions with the solvent and that they can be treated as harmonic oscillators. Some modes such as O–H stretch in the outer-sphere water molecules can be anharmonic,³⁰ but when the reactants and products have similar hydration shells, that is approximately the same number of anharmonic modes, the anharmonic corrections to the thermal functions will cancel.

Thermodynamics of Chelate Ring Closure Reactions. The characteristic feature in chelate complexes is the chelate ring and a model for its formation has been used by Schwarzenbach² to explain the chelate effect. This model is semiquantitative and based on the following two reactions



and



where reaction 34 is a chelate ring closure that can rarely be studied experimentally. The chelate effect can be seen as a result of the much smaller volume (and thereby higher concentration) available to the second donor in reaction 34 than that in reaction 33. From the results given in this work, we are able to make some quantitative statements on the thermodynamics of chelate ring closure reactions. These are relevant for the discussion of mechanisms for inter- and intramolecular ligand exchange reactions as exemplified in one of our previous communications.¹¹

The result that entropy changes for chelate ring opening reactions are more positive when they take place without the mediation of water, than when water participates is consistent with experimental activation entropy data for the ring opening in the $UO_2LF_3^{2-}$ complexes.²⁹ These complexes contain the same donor atoms (N and O), and substituents in the 3 and 5 positions have been used to vary the donor strength of the aromatic nitrogen. The experimental activation entropy, ΔS^\ddagger , for the ring opening when L is 4-(3-pentyl)picolinate, picolinate, and 4-nitropicolinate is -32.8 , -46.7 , and 3.3 J/K·mol, respectively. This indicates that the ring opening for the 4-nitropicolinate complex has less participation of an entering water than in the first two complexes, in agreement with the interpretation of the corresponding rate constants given in ref 29.

The enthalpy of reaction for ring closure reactions has a much larger negative value when the coordination number increases

from four to five and to a smaller extent from five to six, than when the coordination number remains constant. This is presumably a result of the preferred five-coordination of the uranyl(VI) ion.

In one of our previous publications,¹¹ we discussed the mechanism of intramolecular oxalate exchange in $[UO_2(oxalate)_3]^{4-}$ complexes and concluded that the reaction could not take place through a four-coordinated intermediate because of its high activation energy, 82 kJ/mol (mechanism A, Scheme 2 in ref 11); the high activation energy is mainly a result of the unfavorable thermodynamics. The present results show that the thermodynamic barrier is much lower in the water-assisted reaction, 14.5 kJ/mol; hence, we cannot exclude this exchange mechanism. For the ternary complex $[UO_2(oxalate)F_3]^{3-}$, we also investigated the possibility of a water assisted mechanism by optimizing the structure of the five coordinated intermediate $[UO_2(oxalate-uni)(H_2O)F_3]^{3-}$. The energy difference to the precursor is 46.7 kJ/mol, identical to that obtained for the four coordinated intermediate $[UO_2(oxalate-uni)F_3]^{3-}$, cf. ref 11. In a previous study,³¹ we noticed that in binary fluoride uranyl complexes, exchange mechanisms are of dissociative type; the short U–F distances favor a lower coordination number in the intermediate. This argument supports our previous conclusion that the chelate ring opening in the ternary complexes is not water assisted.¹⁰

Chelate ring opening/ring closure is one of the key steps in intra- and intermolecular exchange reactions involving chelating ligands; however, there are very few experimental data and none for the systems we have studied. From the fact that the intramolecular model A results in calculated thermodynamic data that are in good agreement with experiments, we conclude that quantum chemical calculations can also provide reliable estimates of the thermodynamics of other intramolecular reactions such as chelate ring opening/closure. Our results indicate that the entropy change can be used to judge if the chelate ring opening results in decreased or unchanged coordination number; a negative entropy change indicates an unchanged coordination number typical for a water assisted reaction. This thermodynamic result is a useful indicator also for the assignment of mechanisms in ligand exchange reactions.

Acknowledgment. This study has been possible through a grant from the Trygger Foundation, financial support from Deutsche Forschungsgemeinschaft (V.V.). Support from the EU program “ACTAF”, Contract FIKW-CT-2000-00035 is also gratefully acknowledged.

Supporting Information Available: Perspective views of $[UO_2(oxalate-uni)(H_2O)_4]$ (Figure S1); $[Zn(H_2O)_6]^{2+}$, $[Zn(H_2O)_5(NH_3)]^{2+}$, $[Zn(H_2O)_4(NH_3)_2]^{2+}$, $[Zn(H_2O)_4(en)]^{2+}$, $[Zn(H_2O)_4(CH_3NH_2)_2]^{2+}$ (Figure S2); cis- and trans-isomers $[Zn(H_2O)_5(NH_3)]^{2+}$, (H_2O) , $[Zn(H_2O)_6]^{2+}$, $(NH_3)(H_2O)_2$, $[Zn(H_2O)_5(NH_3)]^{2+}$, $(H_2O)_3$, $[Zn(H_2O)_6]^{2+}$, $(NH_3)(H_2O)_5$, $[Zn(H_2O)_5(NH_3)]^{2+}$, $(H_2O)_6$ (Figure S3); $[Zn(H_2O)_6]^{2+}$, (en) , $[Zn(H_2O)_5(en-uni)]^{2+}$, (H_2O) , $[Zn(H_2O)_4(en)]^{2+}$, $(H_2O)_2$ (Figure S4); $UO_2(oxalate)(H_2O)_3$, $[UO_2(oxalate)(oxalate-uni)F]^{3-}$, $[UO_2(oxalate-uni)F_3]^{3-}$, (H_2O) , $[UO_2(oxalate)F_3]^{3-}$, (H_2O) (Figure S5). Geometries (Table S1), entropy data and thermodynamic functions (Table S2), and coordinates (Table S3) of the various Zn(II)-complexes opti-

(29) Szabó, Z.; Grenthe, I. *Inorg. Chem.* **1998**, *37*, 6214.

(30) Chaban, G. M.; Xanthreas, S. S.; Gerber, R. B. *J. Phys. Chem. A* **2003**, *107*, 4952.

(31) Vallet, V.; Wahlgren, U.; Szabó, Z.; Grenthe, I. *Inorg. Chem.* **2002**, *41*, 5626.

mized in the gas phase; geometries (Table S4), data and thermodynamic functions (Tables S5–S6), and coordinates (Table S7) of the binary and ternary uranyl(VI) complexes optimized in the present study; all other structural data have been reported in the Supporting Information of ref 11; entropy

change for the transfer of water in the second coordination sphere to the bulk (Table S8). This material is available free of charge via the Internet at <http://pubs.acs.org>.

JA036646J